Symmetry fractionalization in the topological phase of the spin-$\frac{1}{2}$ J_1-J_2 triangular Heisenberg model

S. N. Saadatmand[*] and I. P. McCulloch

ARC Centre for Engineered Quantum Systems, School of Mathematics and Physics,
The University of Queensland, St. Lucia, Queensland 4072, Australia

Using density-matrix renormalization-group calculations for infinite cylinders, we elucidate the properties of the spin-liquid phase of the spin-$\frac{1}{2}$ J_1-J_2 Heisenberg model on the triangular lattice. We find *four* distinct ground states characteristic of a nonchiral, Z_2 topologically ordered state with vison and spinon excitations. We shed light on the interplay of topological ordering and global symmetries in the model by detecting fractionalization of time-reversal and space-group dihedral symmetries in the anyonic sectors, which leads to the coexistence of symmetry protected and intrinsic topological order. The anyonic sectors, and information on the particle statistics, can be characterized by degeneracy patterns and symmetries of the entanglement spectrum. We demonstrate the ground states on finite-width cylinders are short-range correlated and gapped; however, some features in the entanglement spectrum suggest that the system develops gapless spinonlike edge excitations in the large-width limit.

Introduction. Topological phases [1–3] are an intriguing form of quantum matter, which have been challenging theorists for the last two decades. Before then, it was believed that Landau symmetry-breaking theory [4] can explain ordering and phase transitions of matter through (spontaneous) breaking of a Hamiltonian symmetry. However, topological phases can preserve all symmetries and still acquire a finite energy gap. Topological phases fall into two broad categories, "intrinsic topological order" [3] on $D \geqslant 2$ dimensional lattices, and "symmetry protected topological" (SPT) [5,6] order, which can also exist in one dimension (1D). For the former phase, there is no local unitary transformation to smoothly deform the state into a product state without passing through a phase transition, regardless of the existence of symmetries. The canonical example of an intrinsic topological order is the Z_2 ground state of the *toric code* [7]. On the other hand, SPTs are undeformable into product states only if protected by a symmetry. The best studied example is surely the Haldane phase of odd-integer spin chains [5,6], including the ground state of the exactly solved Affleck-Kennedy-Lieb-Tasaki (AKLT) [8] model. A key breakthrough was the realization that anyonic statistics associated with intrinsic topological order corresponds to fractionalization of symmetry. Therefore, when intrinsic topological order is coupled with lattice symmetries, the symmetries themselves fractionalize and lead to SPT ordering [9–11], which is readily detectable in many numerical methods.

In 1973, Anderson [12] conjectured that the spin-$\frac{1}{2}$ triangular Heisenberg model (THM) with antiferromagnetic nearest-neighbor (NN) bonds should stabilize a resonating-valence-bond (RVB) ground state. The failure of analytic and numerical studies [13–16] to find such a state motivates the search for a minimal extension that increases the frustration with a next-nearest-neighbor (NNN) term. The Hamiltonian is

defined as

$$H = J_1 \sum_{\langle i,j \rangle} \mathbf{S}_i \cdot \mathbf{S}_j + J_2 \sum_{\langle\langle i,j \rangle\rangle} \mathbf{S}_i \cdot \mathbf{S}_j, \tag{1}$$

where $\langle i,j \rangle$ ($\langle\langle i,j \rangle\rangle$) indicates the sum over all NN (NNN) bonds. We set $J_1 = 1$ as the unit of the energy henceforth. Previous numerical studies using a range of techniques [15,17–23] have suggested a spin-liquid [1,3] (SL) region, with phase boundaries in the range of $J_2^{\text{low}} \approx 0.05$ [18] up to $J_2^{\text{high}} \approx 0.19$ [17]. Employing finite-size density-matrix renormalization group (DMRG) [24,25] and using fixed aspect-ratio scaling of magnetic order parameters, we find phase boundaries of $0.101(4) \leqslant J_2 \leqslant 0.136(4)$, the calculation of which will be described in more depth in a future work [26]. In this Rapid Communication, we focus on the properties of the SL phase itself. For classical spins, the model has a phase transition at $J_2 = 0.125$ between two magnetically ordered phases [14]. This point roughly coincides with the center of the spin-liquid region for the quantum model, and in this work we focus on $J_2 = 0.125$. While there is nothing forbidding the coexistence of spontaneous symmetry breaking and topological order, the Hastings-Oshikawa-Lieb-Schultz-Mattis theorem [27] in two dimensions (2D) states that the absence of symmetry breaking in a spin-$\frac{1}{2}$ system on even-width cylinders implies that the ground state is a SL with either gapless (algebraic) excitations, or gapped with degenerate ground states and anyonic excitations. Thus the absence of symmetry breaking is a sufficient (but not necessary) condition for a SL. Previous DMRG studies [20,21] have argued for a gapped Z_2 toric-code SL, and have obtained two possible ground states by the presence (absence) of free spins near the boundaries of finite cylinders. However, the properties of these states are unclear, since, depending on the sector chosen, the state may develop chiral order [21], or breaking of $\mathbf{C}_6$ rotational symmetry [20,21,28], leading to a nematic SL. Recent studies [11,29,30] focused on the kagome lattice show that the time-reversal symmetric Z_2 SL can be fully characterized by the symmetry properties of lattices on tori
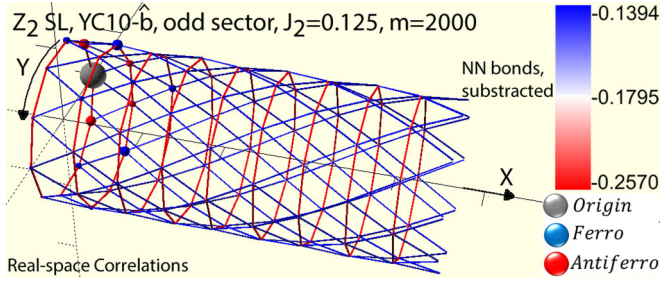
*s.saadatmand@uq.edu.au

FIG. 1. Visualization of the triangular lattice on an infinite YC structure. The size and color of the spheres indicate the long-range correlation with the principal (gray) site. The color of the bonds indicates the strength of the NN correlations. The average of NN correlation is subtracted from each bond to highlight the anisotropy pattern.

or infinite cylinders via the projective symmetry group (PSG) classifications [1,11,29,31,32].

Method. We consider a triangular lattice structure that is wrapped around an infinite cylinder. We employ the infinite matrix product states (iMPS) [25,33,34] ansatz, via the infinite DMRG (iDMRG) algorithm [25,33] with single-site optimization [35] and utilizing $SU(2)$ symmetry to obtain translationally invariant variational ground states on an infinite cylinder. We keep up to $m = 5000$ states, approximately equivalent to 15 000 states of a $U(1)$-symmetric basis. We use the so-called YC structure, where the infinite-length cylinder has a circumference equal to the number of sites in the Y direction, L_y. The mapping of the MPS chain on the cylinder is set to minimize the one-dimensional range of NN and NNN interactions. The setup is shown in Fig. 1, indicating also the correlations of a typical ground state. Bipartite quantities, e.g., reduced density matrix (ρ_r) and entanglement entropy [28], are measured by defining a Y-direction *cut* through the cylinder without crossing any vertical bond. The framework of iDMRG is a natural candidate for calculating symmetry properties, since excitations can be introduced at cylinder edges by manipulating the symmetries of the wave function. Unlike the case for finite systems, the "edges" are effectively at infinity, so they do not affect the translation symmetry of the wave function. The Z_2 SL of the RVB type carries vison excitations, and bosonic and fermionic spinons [36]. We control the even/odd parity of spinon flux in the ground state by setting $SU(2)$ quantum numbers (global spins, S) to be either integers (even sector—no spinon) or odd half integers (odd sector—with spinons) at the unit cell boundary. We cannot directly control the vison flux through the cylinder, so we can only obtain two ground states for each cylinder geometry. However, for finite-L_y cylinders the degeneracy is expected to be lifted, and fortunately we find that the ground states for different width cylinders also give the vison and nonvison sectors, allowing us to obtain all four combinations of even/odd spinons and the presence/absence of a vison flux. We note that Metlitski and Grover [37] and Kolley *et al.* [38] established the observation of a tower of states (TOS) in the low-lying part of the entanglement spectrum (ES) [38,39] as a "smoking gun" evidence for the existence of magnetically ordered states (carrying Nambu-Goldstone excitations). We confirm the nonmagnetic nature of the phase by the absence

of TOS in the ES, regardless of the anyon sector (see below and also Ref. [26]).

We obtain a structure of four anyon sectors of the Z_2 toric-code-type topological order [40] that comprises the identity $\hat{\text{i}}$ anyon (carries no spinon or vison flux), a bosonic spinon $\hat{\text{b}}$ anyon (carries a $S = \frac{1}{2}$ spin), a $\hat{\text{v}}$ anyon (carries a vison and has a π flux threading the cylinder, equivalent to possessing antiperiodic boundary conditions in the Y direction), and finally a fermionic spinon $\hat{\text{f}}$ anyon (a composite excitation, which carries both a $S = \frac{1}{2}$ spin and a π flux). In this Rapid Communication, we work in a minimally entangled states (MES) [41,42] basis introduced in Refs. [11,30] for the four-dimensional ground-state manifold and preserves SPT ordering. For even-L_y cylinders, each unique MES state [11] corresponds to threading an anyonic flux in the long direction and creating a particle/antiparticle pair of â at infinity, namely, $|U_{L_y}^{a/\bar{a}}\rangle$ (also denoted as the YCL_y-â sector). Given a particular MES, the action of a global symmetry group ($\bar{g}$) member Γ_g on the state can be considered as two independent actions on each anyon, i.e., $\Gamma_g|U_{L_y}^{a/\bar{a}}\rangle = \Upsilon_g|U_{L_y}^a\rangle \otimes \Upsilon_{\bar{g}}|U_{L_y}^{\bar{a}}\rangle$, where Υ_g's are unitary operators acting on a single anyon $|U_{L_y}^a\rangle$. Anyons can fractionalize [11,29,30,32] the symmetry $\bar{g}$ by factorizing an identity member of the group (square root of $\bar{g}$). $\bar{g}$ is always a *linear* representation (it is describing a physical symmetry), but Υ_g's can now form a nontrivial PSG, which is a central extension of the original group [1]. In the MPS representation of the ground state, the Υ_g can be expressed as operators acting on the "auxiliary" basis, i.e., the basis of the entanglement Hamiltonian $-\ln(\rho_r)$ on a bipartite cut. Thus the existence of a PSG through measurements of Υ_g's implies 1D SPT ordering [11], by considering rings as single "supersites" (global symmetries along the Y direction are now internal symmetries when viewed as a 1D chain), which is straightforward to detect using iMPS techniques [43].

Ground-state energies. We present ground-state energies of anyonic sectors in Fig. 2. Energies are extrapolated to the thermodynamic limit of basis size $m \to \infty$, using a linear fit against the energy variance per site (see Ref. [28] for details). We suggest that fitting against variances is the most accurate method for extrapolating energies in DMRG (more reliable than extrapolation with respect to the DMRG truncation error). The different topological sectors are expected to acquire slightly different energies on finite-width cylinders. Depending on L_y, we find that the actual ground state in the even/odd sectors varies as to whether or not it contains a π vison flux. In some cases, especially for smaller widths, we have been able to construct variational wave functions in the other sectors by manipulating the wave function (i.e., to force a particular symmetry state), but the resulting states are rather unstable and have considerably higher energies. However, the overall behavior of energies indicates that the difference between energy of even and odd sectors is rapidly decreasing with increasing L_y. This is consistent with having a degenerate ground state in the thermodynamic limit $L_y \to \infty$. Interestingly, there is an energy crossover between even/odd sectors already for YC10, which makes it unreliable to estimate an energy for the $L_y \to \infty$ limit. We note that our energies per site for larger system widths are somewhat lower than previously published results.
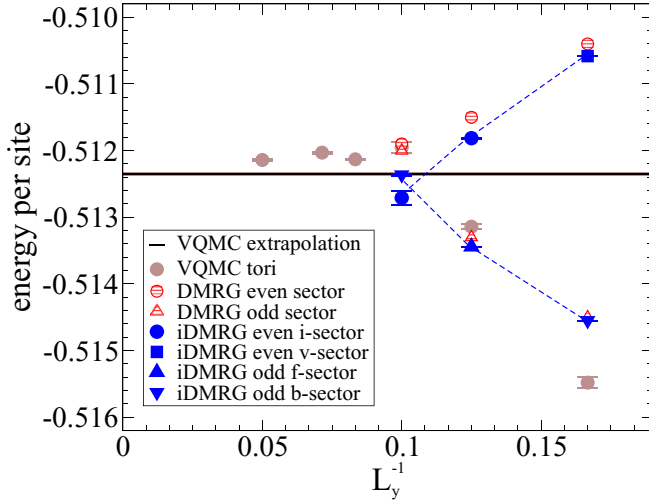
FIG. 2. Ground-state energies at $J_2 = 0.125$ against inverse cylinder width. Our results for infinitely long cylinders with extrapolation to zero variance are in blue. Dashed lines are guides to the eye. Red shaded symbols are finite-size DMRG results from Ref. [21]. Brown symbols are variational quantum Monte Carlo (VQMC) results on $L \times L$ tori with the horizontal line indicating an $L \to \infty$ extrapolation, from Ref. [22].

Symmetry group measurements. We present our main symmetry group measurements on different anyonic sectors and system sizes in Table I. Considering the time-reversal symmetry τ, we find that $|\langle\tau\rangle|$ is very close to 1.0 in all sectors, indicating that time-reversal symmetry is not broken and therefore the ground state is nonchiral. A state carrying a spin-$\frac{1}{2}$ spinon flux can be realized by the action of τ on the auxiliary basis, in the form of $C[\tau^2] = \Upsilon_\tau \Upsilon_\tau^*$. For $\hat{b}$ and $\hat{f}$ sectors, one expects $\langle \Upsilon_\tau \Upsilon_\tau^* \rangle = -1$, antisymmetric under time reversal, which is precisely what we observe (these SPTs are also protected by parity reflection [28]). A state that carries a π vison flux can be detected by the action of the cylinder dihedral symmetry group D_{L_y} in the Y direction. The elements of the group are generated by reflection around a site or bond [28] R_y and a translation by one lattice site T_y. The linear and projective representations can be distinguished by the commutation between R_y and a π rotation, $T_y^\pi = (T_y)^{\frac{L_y}{2}}$. Visons fractionalize D_{L_y}, acquiring an effective antiperiodic boundary condition in the Y direction, whereby reflection

TABLE I. Summary of topological invariants for $L_y \times \infty$ cylinders at $J_2 = 0.125$. $|\langle R_y \rangle|$, $|\langle T_y \rangle|$, and $|\langle \tau \rangle|$ are close to 1.0 in all cases [28].

Structure	Spin-$\frac{1}{2}$ boundary	Degeneracy of ES	$\langle C[D_{L_y}]\rangle$	$\langle C[\tau^2]\rangle$	Sector
YC6	Even	Twofold	-0.999996	1 ± 10^{-11}	$\hat{v}$
YC6	Odd	Twofold	0.9999998	-1 ± 10^{-14}	$\hat{b}$
YC8	Even	Nondegenerate	0.99998	1 ± 10^{-10}	$\hat{\imath}$
YC8	Odd	Fourfold	-0.999990	-1 ± 10^{-11}	$\hat{f}$
YC10	Even	Nondegenerate	0.9996	1 ± 10^{-9}	$\hat{\imath}$
YC10	Odd	Twofold	0.9998	-1 ± 10^{-9}	$\hat{b}$

and π rotations anticommute, $R_y T_y^\pi = -T_y^\pi R_y$. Thus one expects $C[D_{L_y}] = \langle \Upsilon_{R_y} \Upsilon_{T_y^\pi} \Upsilon_{R_y}^\dagger \Upsilon_{T_y^\pi}^\dagger \rangle = -1$ for the $\hat{v}$ and $\hat{f}$ sectors, i.e., D_{L_y} fractionalizes into a PSG with an invariant gauge group [1,11] of Z_2. Combined, the measurements of $C[\tau^2]$ and $C[D_{L_y}]$ give distinct topological invariants for the four sectors, and imply fusion rules [28,40] of a Z_2 SL. Furthermore, this gives information about the self-statistics, in particular, the obtained topological invariants are incompatible [30] with the double-semion topological order [44], since the semion and antisemion are time-reversal partners, but here the two spinon sectors have different PSGs so they cannot be interchanged under τ. We also present a more comprehensive list of symmetry observables in the Supplemental Material [28].

Entanglement spectrum. The ES, set of $\{\lambda_i\}$'s, is a way of presenting the eigenvalues of the entanglement Hamiltonian analogous to a set of energy levels. λ_i can be labeled by any global symmetry of the system as long as it is preserved in the bipartite cut. In this case, we choose $SU(2)$ spin S (preserved explicitly in the calculations), and D_{L_y}, which is *not* preserved exactly, but it is straightforward to diagonalize T_y to obtain the momentum-resolved ES. In the absence of a π vison flux, the allowed Y momenta (k_n's) are arranged with a spacing of $k_n = \frac{2\pi n}{L_y}$. The key difference in the vison sectors is a shift of a half spacing, $k_n = \frac{2\pi}{L_y}(n + 1/2)$, due to the π flux causing an effective antiperiodic boundary condition. Because each anyonic sector corresponds to a unique set of symmetry group measurements that cannot smoothly deform, sectors have a uniquely identifying ES (such a unique form of ES on infinite cylinders was originally observed in the honeycomb Haldane model [45]). In general, it is a nontrivial task to interpret highly populated ES levels, but the overall degeneracy patterns are signatures of SPT ordering, when viewing the cylinder as an infinite chain [6,11,46]. That is, in the presence of SPT, every ES state has a multiple of n-fold degeneracy, where n is determined by the symmetry properties of the state. In particular, the $\hat{\imath}$-sector ES has no degeneracy, the $\hat{b}$ sector has twofold degeneracy associated with half-integer spins (Kramers degeneracy from $C[\tau^2] = -1$), the $\hat{v}$ sector has twofold degeneracy associated with PSGs of D_{L_y}, and the $\hat{f}$ sector has fourfold degeneracy combining Kramers and PSG of D_{L_y}.

In Fig. 3, we present the ES of even-boundary topological sectors for various width cylinders. The $\hat{v}$ sector on YC6 has an exact (up to numerical accuracy) twofold degeneracy arising from $\pm k$ momenta, which is not shared by the $\hat{\imath}$ sector (the $k = 0$ and $k = \pi$ states are nondegenerate), which is a proof for the π flux. The low-lying structure is a deformed two-spinon continuum, most easily seen for the larger-width lattices. We suggest this general pattern [manifested in Fig. 3(c)] is characteristic of even sectors and presumably persists in large-L_y limit.

ES results for odd-boundary topological sectors are presented in Fig. 4. The $\hat{f}$ sector for YC8 has (nearly) fourfold degeneracy and momenta are shifted by $\frac{\pi}{8}$, which indicates both a spinon and vison π flux. The ES of the $\hat{b}$ sector for YC6 or YC10 is (nearly) twofold degenerate due to the odd-half-integer spin boundaries, indicating spinons but no π
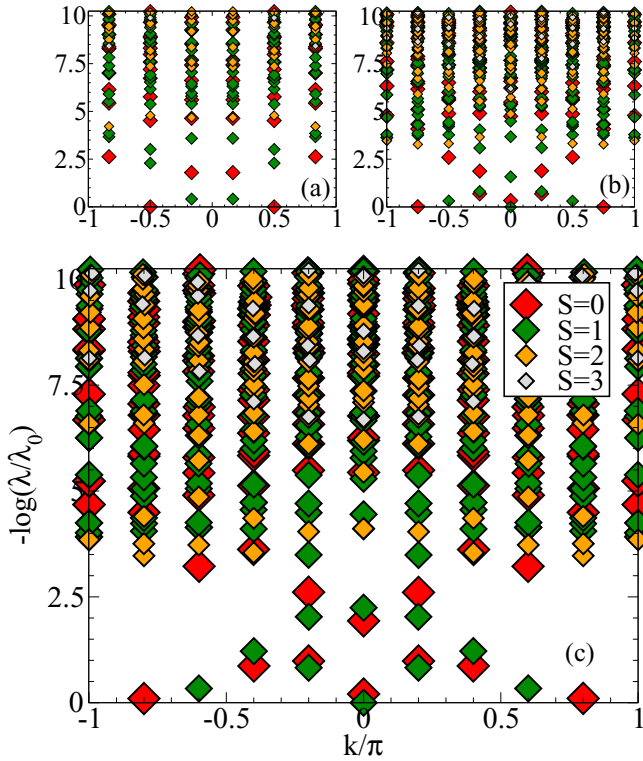
FIG. 3. The momentum-resolved ES of the *even-boundary* topological sectors for different cylinder circumferences L_y, in the spin-liquid region at $J_2 = 0.125$. The topological sectors are (a) YC6-$\hat{v}$, (b) YC8-$\hat{i}$, and (c) YC10-$\hat{i}$.
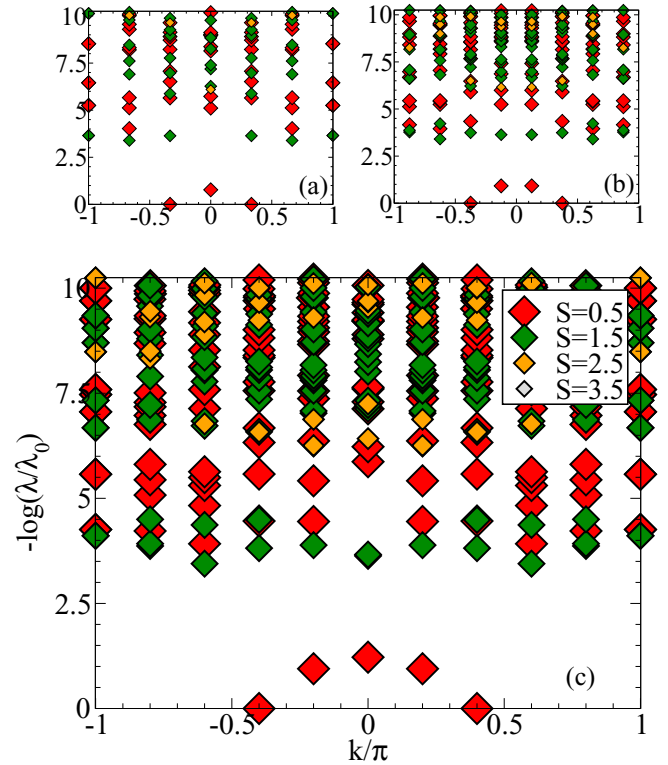

FIG. 4. The momentum-resolved ES of the *odd-boundary* topological sectors for different cylinder circumferences L_y, in the spin-liquid region at $J_2 = 0.125$. The topological sectors are (a) YC6-$\hat{b}$, (b) YC8-$\hat{f}$, and (c) YC10-$\hat{b}$.

flux. Again, the overall pattern of the low-energy structure is consistent between vison and nonvison sectors, and appears to be converging to a well-defined large-L_y limit. Intriguingly, the low-energy structure for the odd sector is reminiscent of a Fermi arc [47], appearing as an excitation mode that only covers a subset of the Brillouin zone.

Hu *et al.* [21] presents ES (not momentum resolved) for two nearly degenerate, YC8 ground states (see Hu *et al.*'s Fig. 5, corresponding to the $\hat{i}$ and $\hat{f}$ sector). Reference [21]'s $\hat{f}$-sector ES is consistent with our Fig. 4(b), however, there is no match between the $\hat{i}$-sector spectra. We suggest Ref. [21]'s $\hat{i}$-sector spectra corresponds to a *chiral state*.

Discussion. Using $SU(2)$-symmetric iDMRG, we have provided a robust demonstration of the properties of the spin-liquid phase of the THM on infinite cylinders, obtaining *four* ground states and their ES degeneracy patterns, which we have classified according to their symmetry fractionalization properties, consistent with theoretical predictions (e.g., see Ref. [11]). We observe dihedral symmetry fractionalization in the model, which shows that the low-lying structure of the THM carries nonchiral Z_2 toric-code-type topological order.

While our calculations are always in the limit of infinite aspect ratio (we do not address directly the nature of the 2D limit), we suggest that the degeneracy of the ground states is robust. We are not yet able to directly measure the energy gap to excited states, however, the iMPS ansatz does readily provide the correlation length, which in all cases is rather small [28], implying a finite gap for finite L_y. However, low-lying

structures in the ES contain some interesting features, such as a Dirac cone (Fig. 3), which will become gapless in the thermodynamic limit. According to edge-ES correspondence for Z_2 topological states enriched by global symmetries [48], the system is likely to have gapless edge states. It is unclear if this would also lead to gapless bulk states, hence we are unable to rule out the possibility that the system is algebraic SL in the 2D limit.

In agreement with Hu *et al.* [21], we observe anisotropic (C_6-symmetry breaking) correlations for the odd sectors only, while the even sectors appear to get isotropic as the width is increased. We were unable to detect the expected topological entanglement entropy of $-\ln(2)$ due to the limited accuracy of the obtained entropy, and relatively small L_y, which is an inherent difficulty with the DMRG procedure [28]. If the system is gapless in the 2D limit, then there will be *logarithmic* corrections that make the fit almost impossible to perform for numerically accessible system sizes.

Irrespective of the nature of the state in the 2D limit, we have shown that finite-width YC structures have short-range correlations and are gapped. A long, narrow cylinder is a plausible geometry for a quantum-engineered device, and there are recent proposals for the construction of the fermionic Hofstadter-Hubbard model on a cylindrical optical lattice [49]. Candidate materials that could be realizations of the Z_2 RVB SL are κ-(BEDT-TTF)$_2$Cu$_2$(CN)$_3$ [50] (with no indication of gapless spin excitations) and EtMe$_3$Sb[Pd(dmit)$_2$]$_2$ [51] (recognized as a gapless state).

[1] X.-G. Wen, Phys. Rev. B **65**, 165113 (2002).

[2] X.-G. Wen, *Quantum Field Theory of Many-Body Systems: From the Origin of Sound to an Origin of Light and Electrons*, Oxford Graduate Texts (Oxford University Press, Oxford, UK, 2007).

[3] X. Chen, Z.-C. Gu, and X.-G. Wen, Phys. Rev. B **82**, 155138 (2010).

[4] L. D. Landau, Phys. Z. Sowjetunion **11**, 26 (1937); V. L. Ginzburg and L. D. Landau, Zh. Eksp. Teor. Fiz. **20**, 1064 (1950); English versions are available in L. D. Landau, *Collected Papers* (Elsevier, Amsterdam, 2013).

[5] Z.-C. Gu and X.-G. Wen, Phys. Rev. B **80**, 155131 (2009).

[6] F. Pollmann, A. M. Turner, E. Berg, and M. Oshikawa, Phys. Rev. B **81**, 064439 (2010); F. Pollmann, E. Berg, A. M. Turner, and M. Oshikawa, *ibid.* **85**, 075125 (2012).

[7] A. Yu. Kitaev, Ann. Phys. **303**, 2 (2003); A. Kitaev and C. Laumann, arXiv:0904.2771.

[8] I. Affleck, T. Kennedy, E. H. Lieb, and H. Tasaki, Phys. Rev. Lett. **59**, 799 (1987); Commun. Math. Phys. **115**, 477 (1988).

[9] A. Mesaros and Y. Ran, Phys. Rev. B **87**, 155115 (2013); M. Barkeshli, M. Bonderson, M. Cheng, and Z. Wang, arXiv:1410.4540.

[10] Y.-C. He, D. N. Sheng, and Y. Chen, Phys. Rev. B **89**, 075110 (2014).

[11] M. P. Zaletel, Y.-M. Lu, and A. Vishwanath, arXiv:1501.01395.

[12] P. W. Anderson, Mater. Res. Bull. **8**, 153 (1973).

[13] D. A. Huse and V. Elser, Phys. Rev. Lett. **60**, 2531 (1988); Th. Jolicoeur and J. C. Le Guillou, Phys. Rev. B **40**, 2727(R) (1989); R. Deutscher and H. U. Everts, Z. Phys. B **93**, 77 (1993); B. Bernu, P. Lecheminant, C. Lhuillier, and L. Pierre, Phys. Rev. B **50**, 10048 (1994); L. Capriotti, A. E. Trumper, and S. Sorella, Phys. Rev. Lett. **82**, 3899 (1999); S. R. White and A. L. Chernyshev, *ibid.* **99**, 127004 (2007); D. J. J. Farnell, O. Götze, J. Richter, R. F. Bishop, and P. H. Y. Li, Phys. Rev. B **89**, 184407 (2014).

[14] Th. Jolicoeur, E. Dagotto, E. Gagliano, and S. Bacci, Phys. Rev. B **42**, 4800(R) (1990); A. V. Chubukov and Th. Jolicoeur, *ibid.* **46**, 11137 (1992).

[15] P. H. Y. Li, R. F. Bishop, and C. E. Campbell, Phys. Rev. B **91**, 014426 (2015).

[16] S. N. Saadatmand, B. J. Powell, and I. P. McCulloch, Phys. Rev. B **91**, 245119 (2015).

[17] L. O. Manuel and H. A. Ceccatto, Phys. Rev. B **60**, 9489 (1999).

[18] R. V. Mishmash, J. R. Garrison, S. Bieri, and C. Xu, Phys. Rev. Lett. **111**, 157203 (2013).

[19] R. Kaneko, S. Morita, and M. Imada, J. Phys. Soc. Jpn. **83**, 093707 (2014).

[20] Z. Zhu and S. R. White, Phys. Rev. B **92**, 041105(R) (2015).

[21] W.-J. Hu, S.-S. Gong, W. Zhu, and D. N. Sheng, Phys. Rev. B **92**, 140403(R) (2015).

[22] Y. Iqbal, W.-J. Hu, R. Thomale, D. Poilblanc, and F. Becca, Phys. Rev. B **93**, 144411 (2016).

[23] A. Wietek and A. M. Läuchli, arXiv:1604.07829.

[24] S. R. White, Phys. Rev. Lett. **69**, 2863 (1992); Phys. Rev. B **48**, 10345 (1993); I. P. McCulloch, J. Stat. Mech. (2007) P10014.

[25] U. Schollwöck, Ann. Phys. (NY) **326**, 96 (2011).

[26] S. N. Saadatmand and I. P. McCulloch (unpublished).

[27] E. Lieb, T. Schultz, and D. Mattis, Ann. Phys. (NY) **16**, 407 (1961); M. Oshikawa, Phys. Rev. Lett. **84**, 1535 (2000); M. B. Hastings, *ibid.* **93**, 140402 (2004); Phys. Rev. B **69**, 104431 (2004); Europhys. Lett. **70**, 824 (2005).

[28] See Supplemental Materials at http://link.aps.org/supplemental/10.1103/PhysRevB.94.121111 for more details on variational energies, numerical convergence of the ES, symmetry group measurements, entanglement entropy, lattice visualization of the even sectors, bond anisotropies, correlation lengths, and the scalar chiral order parameter.

[29] Y. Qi and L. Fu, Phys. Rev. B **91**, 100401(R) (2015).

[30] M. P. Zaletel and A. Vishwanath, Phys. Rev. Lett. **114**, 077201 (2015).

[31] Y. Huh, M. Punk, and S. Sachdev, Phys. Rev. B **84**, 094419 (2011).

[32] A. M. Essin and M. Hermele, Phys. Rev. B **87**, 104406 (2013).

[33] I. P. McCulloch, arXiv:0804.2509.

[34] F. Verstraete, J. I. Cirac, and V. Murg, Adv. Phys. **57**, 143 (2008); L. Michel and I. P. McCulloch, arXiv:1008.4667.

[35] C. Hubig, I. P. McCulloch, U. Schollwöck, and F. A. Wolf, Phys. Rev. B **91**, 155115 (2015).

[36] T. Senthil and M. P. A. Fisher, Phys. Rev. B **62**, 7850 (2000).

[37] M. A. Metlitski and T. Grover, arXiv:1112.5166.

[38] F. Kolley, S. Depenbrock, I. P. McCulloch, U. Schollwöck, and V. Alba, Phys. Rev. B **88**, 144426 (2013).

[39] H. Li and F. D. M. Haldane, Phys. Rev. Lett. **101**, 010504 (2008).

[40] A. Kitaev, Ann. Phys. **321**, 2 (2006).

[41] Y. Zhang, T. Grover, A. Turner, M. Oshikawa, and A. Vishwanath, Phys. Rev. B **85**, 235151 (2012).

[42] H.-C. Jiang, Z. Wang, and L. Balents, Nat. Phys. **8**, 902 (2012).

[43] F. Pollmann and A. M. Turner, Phys. Rev. B **86**, 125441 (2012).

[44] M. Freedman, C. Nayak, K. Shtengel, K. Walker, and Z. Wang, Ann. Phys. **310**, 428 (2004).

[45] L. Cincio and G. Vidal, Phys. Rev. Lett. **110**, 067208 (2013).

[46] A. M. Turner, F. Pollmann, and E. Berg, Phys. Rev. B **83**, 075102 (2011).

[47] X. Wan, A. M. Turner, A. Vishwanath, and S. Y. Savrasov, Phys. Rev. B **83**, 205101 (2011).

[48] W. W. Ho, L. Cincio, H. Moradi, D. Gaiotto, and G. Vidal, Phys. Rev. B **91**, 125119 (2015).

[49] M. Lacki, H. Pichler, A. Sterdyniak, A. Lyras, V. E. Lembessis, O. Al-Dossary, J. C. Budich, and P. Zoller, Phys. Rev. A **93**, 013604 (2016).

[50] Y. Shimizu, K. Miyagawa, K. Kanoda, M. Maesato, and G. Saito, Phys. Rev. Lett. **91**, 107001 (2003); Y. Kurosaki, Y. Shimizu, K. Miyagawa, K. Kanoda, and G. Saito, *ibid.* **95**, 177001 (2005);

M. Yamashita, N. Nakata, Y. Kasahara, T. Sasaki, N. Yoneyama, N. Kobayashi, S. Fujimoto, T. Shibauchi, and Y. Matsuda, Nat. Phys. **5**, 44 (2009).

[51] T. Itou, A. Oyamada, S. Maegawa, M. Tamura, and R. Kato, J. Phys.: Condens. Matter **19**, 145247 (2007); Phys. Rev. B **77**, 104413 (2008).